Ni and Ni–nickel oxide nanoparticles with different shapes and a core–shell structure

Bibhuti B. Nayak [a], Satish Vitta [a,*], A.K. Nigam [b], D. Bahadur [a]

[a] *Department of Metallurgical Engineering and Materials Science, Indian Institute of Technology Bombay, Mumbai 400 076, India*
[b] *Tata Institute of Fundamental Research, Mumbai 400 005, India*

Abstract

Ni nanoparticles with different shapes and having a core–shell structure of Ni–nickel oxide have been prepared by a combination of chemical and gaseous reduction. The first step involves chemical reduction of nickel chloride in an aqueous medium with sodium borohydride ($NaBH_4$). In the second step, the as prepared Ni-complex is reduced further in the presence of 2% H_2 and 98% Ar gas mixture at different temperatures ranging from 550 °C to 850 °C. For gaseous reduction temperatures up to 750 °C, structural studies done at room temperature indicate a core–shell structure of Ni–Ni-oxide whereas for reduction at 850 °C, essentially a single phase of Ni is seen. The particle size ranges from 20 to 120 nm with different shapes for the particles: spherical, ellipsoidal, cylindrical, hexagonal, and polyhedral. The electrical resistivity in all the cases exhibits a typical metallic behavior and the absolute resistivity decreases with increasing gaseous reduction temperature, indicating a progressive reduction of Ni-oxide. The magnetization studied as a function of temperature and field shows a clear core–shell behavior: very high magnetization saturation fields and thermal hysteresis of magnetization.

Keywords: Core–shell structure; Nanoparticles; Magnetism; Nickel

1. Introduction

Synthesis of ferromagnetic nanoparticles with various sizes and shapes and a core–shell structure has received considerable interest in recent years due to their technological interest [1–9]. Magnetic and electrical transport characteristics in principle can be tailored by changing the relative dimensions of the core and shell, their composition and hence magnetic structure. The synthesis of nanoscale pure metallic materials is difficult as it is often accompanied by a spontaneous oxidation of the surface. This tendency for surface oxidation however results in the formation of an interesting class of materials called 'core–shell structures' which have unusual magnetic properties [10–12]. The magnetic behavior varies depending on the nature of shell, which can be antiferromagnetic, paramagnetic, or diamagnetic.

In the present work, differently shaped Ni nanoparticles with nickel oxide as the shell have been synthesized by a combination of chemical and gaseous reduction processes. Structural, electrical and magnetic properties of these nanoparticles are studied in detail.

2. Experimental details

Ni nanoparticles with an oxide shell and different shapes were synthesized by aqueous and gas reduction. The first stage involves precipitation of the Ni-complex particles from an aqueous salt solution of nickel chloride by a reducing agent such as sodium borohydride, $NaBH_4$. In the second stage, the as prepared Ni-complex powders are reduced at different temperatures in the presence of 2% H_2 and 98% Ar gas mixture. The two precursor solutions, 1 M $NiCl_2{\cdot}6H_2O$ and 2 M $NaBH_4$, where M is the molarity of the salt, were prepared separately. $NiCl_2$ solution had an initial pH of 5.1 while the 2 M $NaBH_4$ solution has a pH of 9.7. The by-products of reduction reaction, NaCl and H_3BO_3 remain dissolved and they were removed by repeated centrifuging and washing with distilled water. The centrifuged product was dried under lamp. Pellets were made (from the as prepared powders) at a constant pressure of 75 kg/cm^2 and reduced at temperatures between 550 °C and 850 °C for 1 h. Structural studies of the reduced

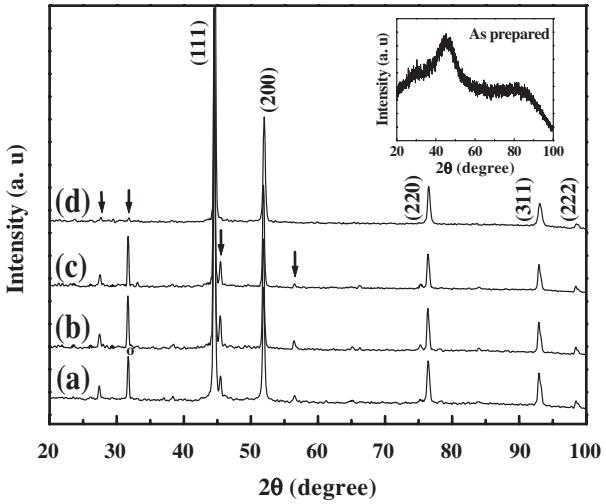

Fig. 1. X-ray diffraction pattern from Ni-complex powder reduced at 550 °C (a), 650 °C (b), 750 °C (c) and 850 °C (d) for 1 h in presence of 2% H_2 and 98% Ar gas mixture. Arrows indicate peaks corresponding to the Ni-oxide phase which decrease in intensity as the reduction temperature increases. Inset shows a broad peak from the as prepared powder.

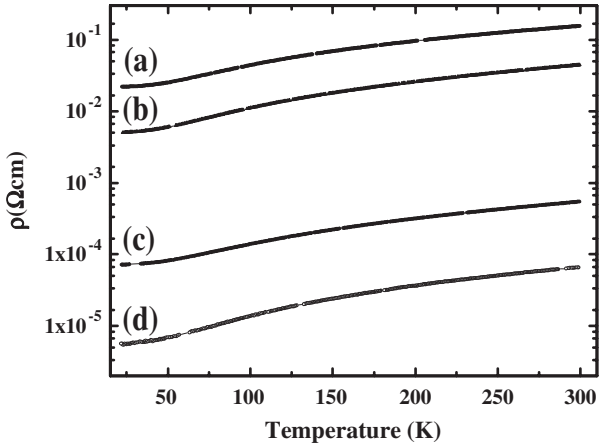

Fig. 3. The electrical resistivity as a function of temperature shows a typical metallic behavior for all the Ni–Ni-oxide structures obtained by reduction at different temperatures: (a) 550 °C, (b) 650 °C, (c) 750 °C and (d) 850 °C.

powder were done by X-ray diffraction and transmission electron microscopy. Resistivity was measured by the standard four-probe technique and the magnetization was studied using vibrating sample magnetometer (VSM).

3. Results and discussion

Fig. 1(a–d) shows the X-ray diffraction patterns after reduction for 1 h at different temperatures: 550 °C, 650 °C, 750 °C and 850 °C. The X-ray diffraction pattern of as-prepared powder (inset of Fig. 1) has a single broad peak at ~45° 2θ corresponding to (111) reflection position of Ni. This clearly shows that Ni in the as-prepared powder is in a crystalline cluster form with a size of ~3 nm.

Reducing the as prepared Ni powder at 550 °C in 2% H_2+98% Ar gas mixture leads to growth of the crystalline Ni clusters as well as development of Ni-oxide shell as seen in Fig. 1 (a). Increasing the reduction temperature up to 750 °C retains the core-Ni/shell-Ni-oxide structure as seen from Fig. 1(b) and (c). Gaseous reduction at 850 °C however results in near complete elimination of the Ni-oxide shell as seen in Fig. 1(d). The XRD pattern shows the presence of Ni with almost no peaks corresponding to Ni-oxide. The crystallite size of Ni is determined using Debye Scherrer relation, and is found to be around 50–75 nm indicating no significant grain growth as the reduction temperature increases from 550 to 850 °C.

Different shapes of nanograin Ni particles with a Ni-oxide shell structure were observed by transmission electron microscopy (Fig. 2). The shape of the particles varies from nearly spherical to cylindrical, hexagonal, ellipsoidal, and polyhedral. The average particle size varies from 20 to 120 nm for all the samples in agreement with X-ray results. The different shapes however were present in powders reduced at different temperatures indicating that the growth habitat is independent of temperature.

The electrical resistivity as a function of temperature of the Ni–Ni-oxide core–shell structure is shown in Fig. 3. A typical metallic behavior is observed in all the cases. The absolute resistivity decreases with increasing reduction temperature due to decreasing volume fraction of minor phase (Ni-oxide) in the system. The resistivity of nickel reduced at 850 °C is still higher than the bulk value by an order of magnitude. The high value of resistivity is due to grain boundary scattering from Ni nanoparticles as well as due to the presence of small quantities of Ni-oxide.

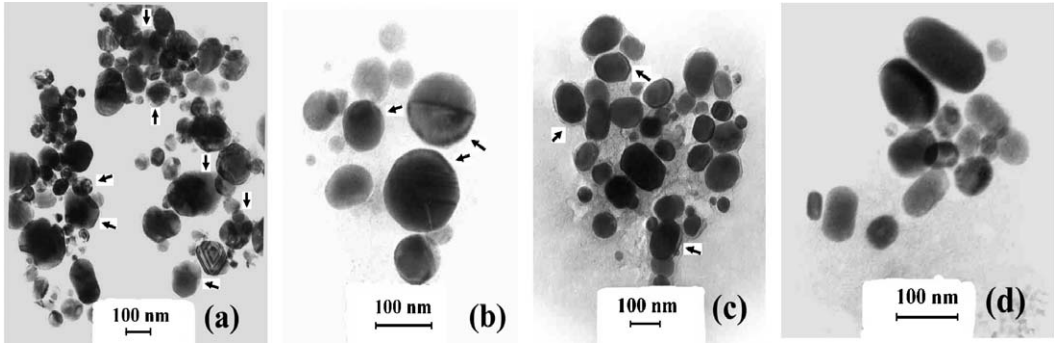

Fig. 2. TEM micrographs of Ni particles reduced at annealing temperatures of 550 °C (a), 650 °C (b), 750 °C (c) and 850 °C (d). Arrow indicates Ni-oxide shell on a Ni particle.

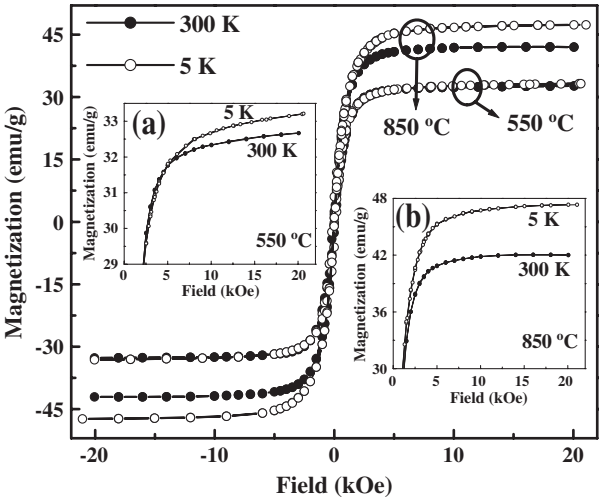

Fig. 4. The magnetization of Ni nanoparticles and Ni–Ni-oxide core–shell structures as a function of external field indicates different saturation behavior for reduction at 550 °C (inset (a)) and 850 °C (inset (b)).

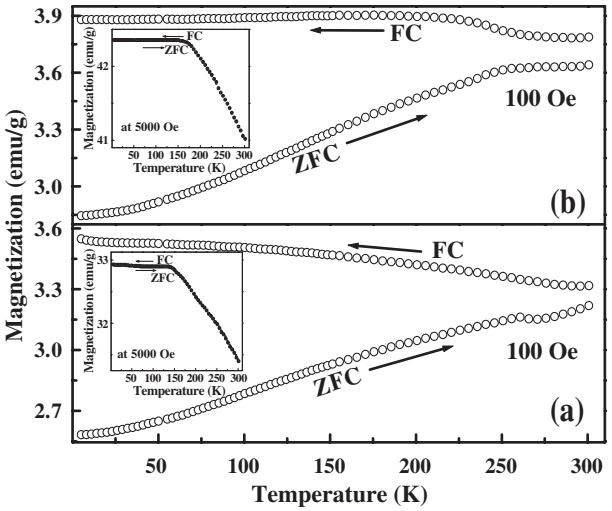

Fig. 5. Temperature dependence of magnetization of Ni nanoparticles and Ni–Ni-oxide core–shell structure in a field of 100 Oe shows thermal hysteresis. The hysteresis behavior vanishes at 5000 Oe (insets). The reduction temperature is 550 °C (a) and 850 °C (b).

The magnetization M as a function of external field H at room temperature, 300 K and 5 K is shown in Fig. 4. The magnetization near saturation, at an external field of 20 kOe, for the Ni nanoparticles obtained after reduction at 850 °C is higher compared to that obtained after 550 °C reduction. This is due to the presence of relatively higher Ni-oxide in the form of a shell around Ni-core after reduction at 550 °C compared to 850 °C. A closer look at the magnetization at high fields, insets in Fig. 4, supports the presence of higher Ni-oxide after reduction at 550 °C. The magnetization at 5 K does not reach saturation even at external fields of 20 kOe in the presence of thick Ni-oxide shell layer. The saturation magnetization of Ni obtained after reduction at 850 °C however is still lower than the equivalent bulk value due to the nanosize as well as the presence of small amounts of oxide.

The magnetization data of Ni–nickel oxide nanostructures along with that of pure bulk nickel are given in Table 1. The coercivity H_c of Ni–Ni-oxide structure obtained after reduction at 550 °C increases with decreasing temperature from ~80 Oe at 300 K to 145 Oe at 5 K. The coercivity of nearly pure Ni nanoparticles obtained by reduction at 850 °C however remains a constant at ~21 Oe both at 300 K and 5 K. The Ni-oxide, NiO, is known to be antiferromagnetic and when present as a shell on the ferromagnetic Ni-core, pins the magnetization. At low temperatures, 5 K, a large external field H will be required to reverse the magnetization direction leading to an increase in the coercivity value compared to room temperature.

Table 1
Magnetization data of Ni–Ni-oxide nanostructures along with pure bulk Ni

Sample	At 300 K		At 5 K		Blocking temperature (T_B, K)
	H_c (Oe)	M_s (emu/g) at 20000 Oe	H_c (Oe)	M_s (emu/g) at 20000 Oe	
Ni_550	80	32.5	145	33	>300
Ni_850	21.4	42.2	21	47.1	>300
Bulk Ni [13]	100	55	–	–	–

The variation of magnetization with temperature in the range 5–300 K in an external field of 100 Oe shows a path dependant hysteresis behavior both for the Ni-nanoparticles and Ni–Ni-oxide core-shell structures, Fig. 5. In an external field of 5000 Oe however the hysteresis vanishes completely in both the cases. The presence of hysteresis at low fields and its absence at high fields is a characteristic feature of superparamagnetic behavior, observed in nanosize particles [14,15]. The blocking temperature, T_B, above which the magnetization is independent of the path is found to be >300 K in 100 Oe external field. A broad variation of zero field cooled magnetization indicates the presence of a distribution of particles size, as seen in TEM (Fig. 2).

4. Conclusions

Nanoparticles and core–shell structures of Ni have been synthesized by a combination of chemical and gaseous reduction process. Structural studies show that the particle size ranges from 20 nm to 120 nm. The particles were found to have different shapes (spherical, cylindrical, ellipsoid, hexagonal and polyhedral) independent of gaseous reduction temperatures. The absolute resistivity decreases as temperature of reduction increases and this is due to a decrease in the fraction of insulating phase made of Ni-oxide. The magnetization values are much lower compared to bulk values and it is due to the presence of non-magnetic/antiferromagnetic secondary phase of Ni-oxide. The ZFC and FC magnetization curves at 100 Oe do not superpose and show a blocking temperature T_B above the room temperature whereas if the field is increased to 5000 Oe, the thermal hysteresis behavior of magnetization vanishes, which is typical of superparamagnetic particles. The non-saturating behavior of magnetization at room temperature as well as at 5 K up to 20 kOe external field for the Ni particles obtained by gaseous reduction at 550 °C suggests a shell of Ni-oxide on Ni particles.

Acknowledgements

The authors acknowledge the Dept. of Science and technology, Govt. of India for financial assistance.

References

[1] J.M. Broto, J.C. Ousset, H. Rakoto, S. Askenazy, Ch. Dufor, M. Brieu, P. Mauret, Solid State Commun. 85 (1993) 263.
[2] H. Kisker, T. Gessmann, R. Würschum, H. Kronmüller, H.-E. Schaefer, Nanostruct. Mater. 6 (1995) 925.
[3] H.-E. Schaefer, H. Kisker, H. Kronmüller, R. Würschum, Nanostruct. Mater. 1 (1992) 523.
[4] S. Illy-Cherrey, O. Tillement, J.M. Dubois, F. Massicot, Y. Fort, J. Ghanbaja, S. Bégin-Colin, Mater. Sci. Eng., A 338 (2002) 70.
[5] J.-S. Jung, K.-H. Choi, W.-S. Chae, Y.-R. Kim, J.-H. Jun, L. Malkinski, T. Kodenkandath, W. Zhou, J.B. Wiley, C.J. O'Connor, J. Phys. Chem. Sol. 64 (2003) 385.
[6] M.J. Aus, B. Szpunar, A.M. El-Sherik, U. Erb, G. Palumbo, K.T. Aust, Scr. Metall. Mater. 27 (1992) 1639.
[7] Kh.Ya. Mulyukov, G.F. Korznikova, R.Z. Abdulov, R.Z. Valiev, J. Magn. Magn. Mater. 89 (1990) 207.
[8] B. David, N. Pizúrová, O. Schneeweiss, P. Bezdička, I. Morjan, R. Alexandrescu, J. Alloys Compd. 378 (2004) 112.
[9] N.J. Tang, W. Zhong, H.Y. Jiang, Z.D. Han, W.Q. Zou, Y.W. Du, Solid State Commun. 132 (2004) 71.
[10] L. Savini, E. Bonetti, L.D. Bianco, L. Pasquini, S. Signoretti, P. Allia, M. Coisson, J. Moya, V. Selvaggini, P. Tiberto, F. Vinai, J. Appl. Phys. 91 (2002) 8593.
[11] L. Xiang, Y.P. Yin, Y. Jin, J. Solid State Chem. 177 (2004) 1535.
[12] X. Lu, G. Liang, Z. Sun, W. Zhang, Mater. Sci. Eng., B 117 (2005) 147.
[13] S.-H. Wu, D.-H. Chen, J. Colloid Interface Sci. 259 (2003) 282.
[14] X. Sun, M.J. Yacaman, Mater. Sci. Eng., C 16 (2001) 95.
[15] N. Cordente, B. Toustou, V. Collière, C. Amiens, B. Chaudret, M. Verelst, M. Respaud, J.-M. Broto, C.R. Acad. Sci. Paris, Chimie/Chemistry 4 (2001) 143.